ORIGINAL PAPER
Other Systems of Anomalous Characteristics
www.pss-b.com

Delocalized Nonlinear Vibrational Modes in Graphene: Second Harmonic Generation and Negative Pressure

Elena A. Korznikova, Stepan A. Shcherbinin, Denis S. Ryabov, George M. Chechin, Evgeny G. Ekomasov, Elham Barani, Kun Zhou, and Sergey V. Dmitriev*

With the help of molecular dynamics simulations, delocalized nonlinear vibrational modes (DNVM) in graphene are analyzed. Such modes are dictated by the lattice symmetry, they are exact solutions to the atomic equations of motion, regardless the employed interatomic potential and for any mode amplitude (though for large amplitudes they are typically unstable). In this study, only one- and two-component DNVM are analyzed, they are reducible to the dynamical systems with one and two degrees of freedom, respectively. There exist 4 one-component and 12 two-component DNVM with in-plane atomic displacements. Any two-component mode includes one of the one-component modes. If the amplitudes of the modes constituting a two-component mode are properly chosen, periodic in time vibrations are observed for the two degrees of freedom at frequencies ω and 2ω, that is, second harmonic generation takes place. For particular DNVM, the higher harmonic can have frequency nearly two times larger than the maximal frequency of the phonon spectrum of graphene. Excitation of some of DNVM results in the appearance of negative in-plane pressure in graphene. This counterintuitive result is explained by the rotational motion of carbon hexagons. Our results contribute to the understanding of nonlinear dynamics of the graphene lattice.

1. Introduction

Graphene is carbon two-dimensional crystalline material which has received a great deal of attention due to unique combination of physical and mechanical properties promising for a number of applications.[1–3] In particular, linear and nonlinear dynamics of graphene lattice was extensively studied. Linear phonon dispersion curves of graphene and graphite have been measured and calculated.[4,5] It has been shown experimentally[6] and using ab initio density functional perturbation theory that graphene demonstrates negative linear thermal expansion coefficient in a wide temperature range.[7] Phonon transport in graphene has been investigated with the help of molecular dynamics method to demonstrate a very high thermal conductivity of pristine graphene and a noticeable reduction of thermal conductivity by defects.[8–10] The effects of temperature, strain, and size on the thermal conductivity of suspended graphene have been analyzed in ref. [11]. Graphene supports soliton-like distortions called wrinklons.[12–16] It has been shown that graphene and other sp^2 carbon nanomaterials support nonlinear spatially localized vibrational modes called discrete breathers or intrinsic localized modes.[17–30] The role of such modes in solid state physics is actively discussed.[31,32] Discrete breathers can assist energy transfer to ac driven graphene nanoribbon.[33] Graphene can act as an elastic damper[34]

Recently, with the help of the group theory methods,[35–38] delocalized nonlinear vibrational modes (DNVM), originally called "bushes of nonlinear normal modes," have been derived for the hexagonal lattice[39] (graphene also has hexagonal lattice). This approach takes into account only symmetry of crystal lattice, that is why DNVM are exact solutions to the

Dr. E. A. Korznikova, S. V. Dmitriev
Institute for Metals Superplasticity Problems of the Russian Academy of Sciences
Khalturina St. 39, Ufa 450001, Russia
E-mail: elena.a.korznikova@gmail.com

S. A. Shcherbinin, Dr. D. S. Ryabov, Dr. G. M. Chechin
Southern Federal University
Institute of Physics
Stachki Ave. 194, Rostov-on-Don 344090, Russia

Prof. E. G. Ekomasov
National Research South Ural State University
Lenin Ave. 76, Chelyabinsk 454080, Russia

Prof. E. G. Ekomasov
Tyumen State University
Volodarsky Street 6, Tyumen 625003, Russia

E. Barani
Department of Chemistry, Faculty of Science
Ferdowsi University of Mashhad
Azazi Square V, Mashhad 91775-1436, Iran

Dr. K. Zhou
School of Mechanical and Aerospace Engineering
Nanyang Technological University
50 Nanyang Avenue, Singapore 6397988, Singapore

Prof. S. V. Dmitriev
National Research Tomsk State University
Lenin Ave. 36, Tomsk 634050, Russia

DOI: 10.1002/pssb.201800061

dynamical equations of atomic motion for any amplitude and for any type of interatomic potentials. For large amplitudes DNVM typically become unstable. Dynamics of N-component DNVM can be effectively described by a system with N degrees of freedom.

The study of DNVM is important for at least three reasons. First, in molecular dynamics simulations, DNVM with frequencies outside the phonon band can be used for setting initial conditions suitable for excitation of discrete breathers. This can be done by imposing a localizing function with a few physically motivated parameters on such DNVM. This approach has been used successfully for excitation of new types of discrete breathers in graphene[23] and in two-dimensional Morse lattices.[40] Second, DNVM at sufficiently large amplitudes demonstrate modulational instability which can result in spontaneous formation of discrete breathers.[41–48] Third, it was shown that excitation of DNVM affects elastic properties of the lattice and, in combination with homogeneous tension, can result in appearance of auxeticity of the hexagonal lattice (negativity of its Poisson's ratio).[48]

It should be noted that materials with negative Poisson's ratio, negative thermal expansion, negative compressibility, and other anomalous characteristics attract considerable attention of researchers because they are interesting from the theoretical standpoint and have a potential in applications.[49–77]

In the present study, we investigate dynamics of all possible one-component and two-component DNVM with in-plane atomic vibrations in hexagonal lattice, considering realistic, many-body interatomic potentials for graphene.

2. Simulation Details

Hexagonal lattice of graphene is shown in **Figure 1**. Cartesian coordinate system is used with x (y) axis oriented along the zigzag (armchair) direction. Primitive translational cell includes two carbon atoms, as shown by the dashed lines. In simulations the computational cell that includes 6×6 primitive translational cells is used. Such cell is sufficient to simulate any of the studied DNVM, though for some of them even smaller simulation cell would be sufficient. The simulation cell is subject to periodic boundary conditions.

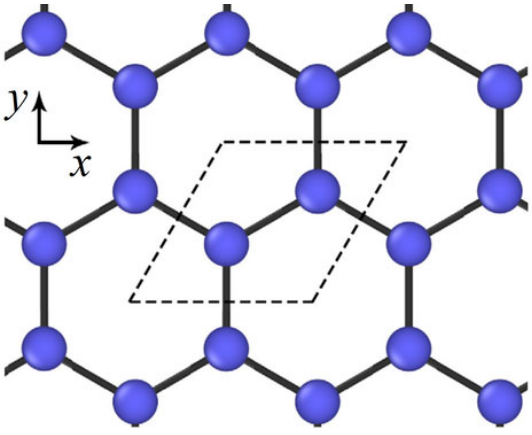

Figure 1. Graphene lattice with zigzag (armchair) direction along x (y) axis. Primitive translational cell is shown by dashed lines.

All the studied DNVM are excited by applying initial displacements to the atoms according to the patterns described in ref. [39] and shown in **Figure 2**. Initial velocities of atoms are equal to zero.

We employ the interatomic potentials developed for graphene by Savin with co-authors.[8] Home made molecular dynamics code is used for NVE ensemble, which means that number of atoms, N, volume, V, and total (kinetic plus potential) energy of the system, E, are conserved. Each atom has three degrees of freedom but, in our simulations, the out-of-plane displacements of the atoms were not observed for the in-plane initial displacements within the simulation run time. That is why constant volume of the system actually means constant area of the two-dimensional computational cell.

The equations of atomic motion are integrated with the use of the Störmer method of sixth order accuracy with the time step of 0.5 fs. This symplectic method is a member of a wider family of integrators, as demonstrated in ref. [78]. Relative change of total energy of the system in a typical numerical run was below 10^{-9}.

Atoms in the studied DNVM perform time-periodic motion. Within one period kinetic energy of the moving atoms vanishes two times, at times t_1 and t_2, when the atoms are at maximal distance from the equilibrium positions. Let the coordinates of particular moving atom at t_1 and t_2 are (x_1, y_1) and (x_2, y_2), respectively. Then DNVM amplitude is calculated as $A = (1/2)\sqrt{(x_2 - x_1)^2 + (y_2 - y_1)^2}$. DNVM period is $T = 2(t_2 - t_1)$ and frequency is $\omega = 1/T$.

Excitation of a DNVM produces time-periodic internal in-plane stresses in graphene, σ_{xx}, σ_{yy}, and σ_{xy}. Averaged over an oscillation period values of stresses are calculated as follows

$$\langle \sigma_{ij} \rangle = \frac{1}{T} \int_0^T \sigma_{ij}(t) dt. \quad (1)$$

Averaged over time pressure can be found as

$$\langle p \rangle = -\frac{1}{2} \left(\langle \sigma_{xx} \rangle + \langle \sigma_{yy} \rangle \right). \quad (2)$$

Since the shape and size of the computational cell were fixed, we could only calculate the time-averaged in-plane pressure as given by Equations (1) and (2) but not the equilibrium area of the computational cell. Some of the studied modes produce positive pressure but there are the modes producing negative pressure. In order to calculate equilibrium area of the computational cell one has to allow expansion or contraction of the cell to keep zero stresses. This problem was not considered in our study.

3. Results and Discussion

Here we discuss the results of molecular dynamics simulations of all one- and two-component DNVM in graphene.

There exist four one-component and twelve two-component DNVM,[39] all of them are shown in Figure 2. The four one-

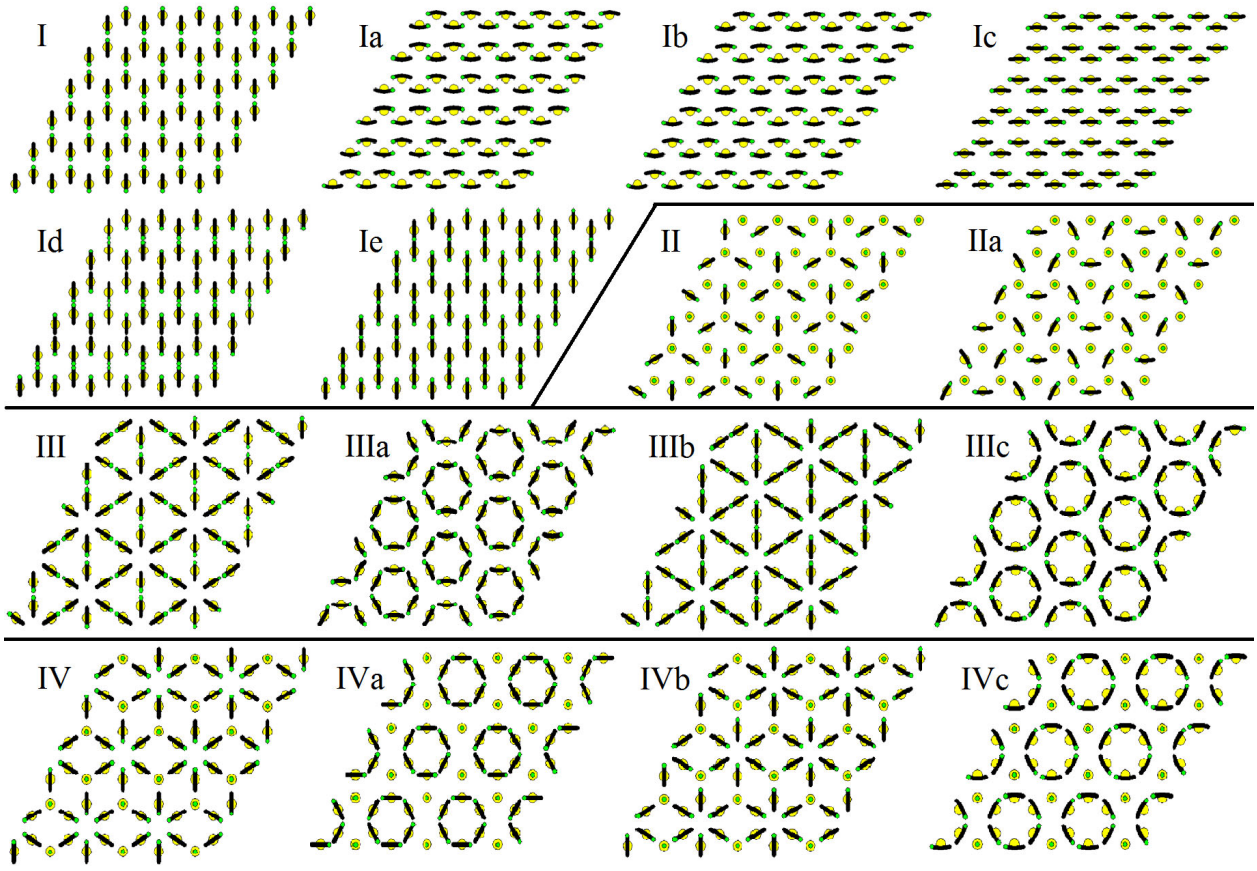

Figure 2. Delocalized nonlinear vibrational modes supported by hexagonal lattice of graphene.[39] Yellow circles show the unperturbed hexagonal lattice points. Trajectories of the atoms are shown by the black lines. Small green dots correspond to the atomic positions at the time when they are at maximal distance from the lattice points. Modes I, II, III, and IV are one-component DNVM and the other modes are two-component DNVM. Modes Ia to Ie include mode I. Similarly, mode IIa includes mode II, modes IIIa to IIIc include mode III, and modes IVa to IVc include mode IV.

component DNVM are labeled with Roman numerals from I to IV. The two-component modes are divided into four groups related to each one-component mode and they are labeled with a Roman numeral and a Latin letter. Yellow circles in Figure 2 show the points of the unperturbed hexagonal lattice. Black lines show the trajectories of the atoms near the lattice points. Small green dots correspond to the atomic positions at the time when they are at maximal distance from the lattice sites.

In the following, first we report the frequency-amplitude and pressure-amplitude dependencies for the one-component modes. Then we show that all the two-component DNVM demonstrate the phenomenon of second harmonic generation. Finally, the effect of negative pressure induced in the graphene sheet by excitation of particular two-component DNVM is discussed.

3.1. One-Component DNVM

One-component DNVM are essentially single degree of freedom vibrational modes. Initial displacements of the atoms according to the patterns shown for DNVM I, II, III, and IV in Figure 2 by green dots immediately produce the exact vibrational modes. In

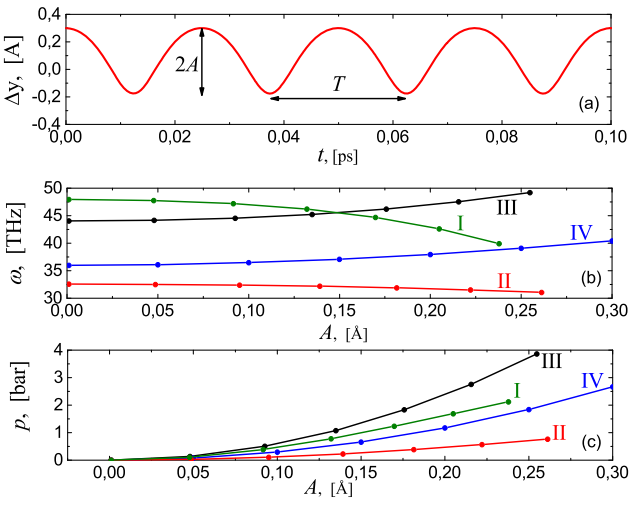

Figure 3. a) Displacement Δy as the function of time for one atom of DNVM I. The mode amplitude is $A = 0.238$ Å, period is $T = 0.0250$ ps, and frequency $\omega = 1/T = 39.9$ THz. b) Frequency as the function of amplitude for the one-component DNVM from I to IV. c) Pressure as the function of amplitude for the one-component DNVM from I to IV.

Figure 3a we plot as the function of time the displacement Δy of one atom for DNVM I. Displacement varies in time not sinusoidally, reflecting anharmonicity of the mode. The mode amplitude A and period T are defined in this plot (see also Section 2 for the definitions of A and T). DNVM frequency is $\omega = 1/T$. Particularly, for this example, $A = 0.238$ Å, $T = 0.0250$ ps, and $\omega = 39.9$ THz.

In Figure 3b frequency as the function of amplitude is shown for all four one-component DNVM. It can be seen that DNVM I and II demonstrate soft-type nonlinearity (decrease of ω with increasing A), while DNVM III and IV are characterized by the hard-type nonlinearity, with frequency growing with amplitude. DNVM frequencies can be compared with the highest phonon frequency of graphene, which is at about 48 THz. Thus, all DNVM have frequencies within the phonon band and only DNVM III at very large amplitudes leaves the phonon spectrum.

In Figure 3c pressure as the function of amplitude is shown for all four one-component DNVM. As can be expected, all one-component DNVM produce positive pressure that increases with A.

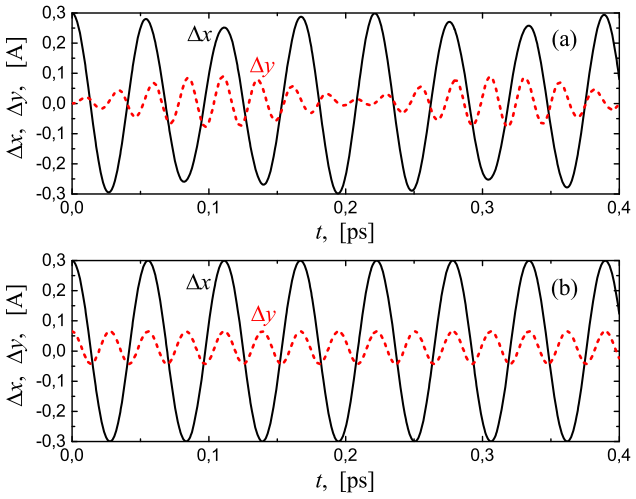

Figure 5. a) Displacements of the atom circled in Figure 4a as the functions of time for hypothetical mode X excited with the initial amplitude $A_X = 0.3$ Å. b) Displacements of the atom circled in Figure 4c as the functions of time for DNVM IIIa excited with the amplitudes $A_X = 0.3$ Å and $A_{III} = 0.065$ Å.

3.2. Two-Component DNVM. Second Harmonic Generation

Two-component DNVM are two degree of freedom vibrational modes. Let us show the relation between one-component and two-component modes considering, as an example, the one-component mode III and two-component mode IIIa (these modes can be found in the third row of Figure 2). To do so, we excite the vibrational mode according to the pattern of initial displacements shown in **Figure 4**a, let us call it mode X. Here each atom is displaced by the vector having length $A_X = 0.3$ Å, which is the mode amplitude. For the atom circled in Figure 4a we calculate the components of its displacement vector as the functions of time, $\Delta x(t)$ and $\Delta y(t)$ and plot them in **Figure 5**a. It can be seen that in addition to the main $\Delta x(t)$ oscillation component a small $\Delta y(t)$ component appears and that the vibration is not periodic. From the theoretical consideration[39] it follows that excitation of mode X inevitably excites the additional DNVM III. We then combine the mode X with DNVM III and find that for the mode amplitudes $A_X = 0.3$ Å $A_X = 0.3$ Å and $A_{III} = 0.065$ Å periodic motion is realised, see Figure 5b, and this periodic mode is the two-component DNVM IIIa.

Having the above picture in mind, we now describe how to initiate a two-component DNVM in the molecular dynamics simulations. To do so, one has to sum up the initial displacements of the atoms according to the patterns shown by the green dots in Figure 2 for the one-component and two-component modes. Namely, the patterns Ia to Ie are summed up with the pattern I in order to excite the modes Ia to Ie. Similarly, the pattern IIa is summed up with the pattern II; the patterns IIIa to IIIc are summed up with the pattern III; and the patterns IVa to IVc are summed up with the pattern IV. The amplitudes of the two modes to be mixed should be chosen such that a periodic motion takes place, as exemplified in Figure 5b for mixing the modes III and IIIa.

Note that DNVM IIIa has frequency $\omega = 18.0$ THz for the main Δxt component and double frequency for the $\Delta y(t)$ component, which is the effect of the second harmonic generation, see Figure 5b.

In fact, any two-component DNVM includes a one-component DNVM with properly chosen amplitude to achieve a

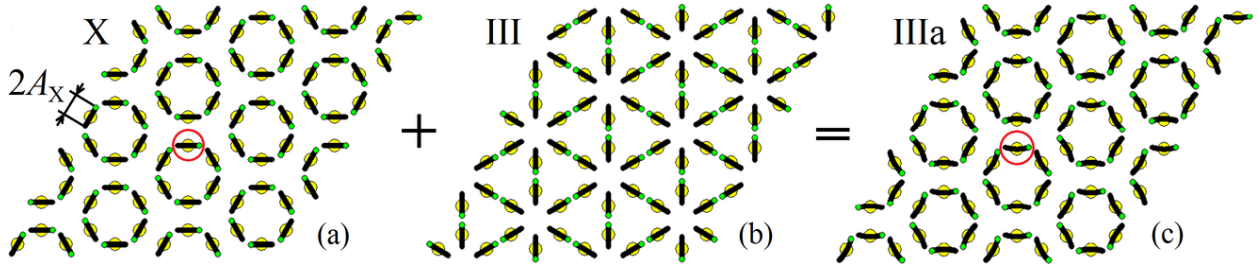

Figure 4. a) Hypothetical vibrational mode X of amplitude A_X. Displacements of the circled atom as the functions of time are shown in Figure 5a. b) One-component DNVM III. c) Two-component DNVM IIIa obtained by superposition of mode X and DNVM III with the amplitudes $A_X = 0.3$ Å and $A_{III} = 0.065$ Å. Displacements of the circled atom as the functions of time are shown in Figure 5c.

periodic motion. In graphene, this one-component DNVM always has a smaller amplitude and frequency two times greater than the main vibrational mode frequency. Thus, any two-component DNVM generates the second harmonic.

In some cases the second harmonic can have frequencies well above the maximal phonon frequency. For instance, DNVM Ia with main amplitude 0.15 Å and main frequency $\omega = 46.3$ THz has amplitude of DNVM I $A_I = -0.0163789$ Å and frequency $\omega = 92.6$ THz, which is nearly as twice as the maximal phonon frequency.

DNVM are natural vibrational modes of graphene lattice and the existence of the natural vibrations at frequencies considerably above the maximal phonon frequency is, in our opinion, an interesting finding. Second harmonic generation is a nonlinear effect, since the amplitude of the second harmonic rapidly (quadratically) decreases with decreasing amplitude of the main mode.

3.3. Two-Component DNVM. Negative Pressure

As it was shown in Section 3.1, the excitation of one-component DNVM produces a positive in-plane pressure in graphene sheet, see Figure 3c. While most of the two-component DNVM also produce positive pressure, there are two exceptional DNVM, namely IIIa and IVa, which produce *negative* pressure. In **Figure 6**, as the functions of main mode amplitude we plot a) the amplitude of additional DNVM III; (b) frequency; and c) pressure. These quantities are calculated as follows. First, for chosen main amplitude A of mode IIIa one finds the amplitude of mode III, A_{III}, such that a periodic motion is observed. An example for $A = 0.3$ Å is given in Figure 5b, where it was shown that in this case $A_{III} = 0.065$ Å. The dependence of A_{III} on A, when periodic motion is observed, is plotted in Figure 6a. It can be seen that $A_{III} \sim A^2$. The main mode frequency ω is calculated from Figure 5b for the main displacement oscillation $\Delta x(t)$ and it is shown as the function of A in Figure 6b. The additional mode

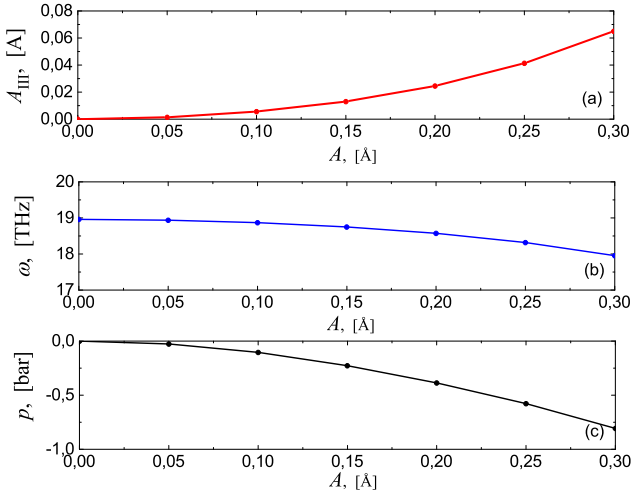

Figure 6. Characteristics of DNVM IIIa as the functions of the main mode amplitude: (a) amplitude of the additional DNVM III, (b) frequency, (c) pressure.

III oscillates with frequency 2ω, see displacement $\Delta y(t)$ in Figure 5b. Pressure p for particular A is calculated with the help of Equations (1) and (2). Pressure as the function of A is plotted in Figure 6c.

It can be seen from Figure 6c that pressure is negative for DNVM IIIa and similar result was found for DNVM IVa. DNVM IIIa and IVa produce negative pressure because of particular pattern of atomic displacements, in both these modes one can see rotation of hexagons (Figure 2). Indeed, looking at the patterns of atomic displacements of modes IIIa and IVa in Figure 2, one can see that the green dots, showing the atomic positions at the time when they are at maximal distance from the lattice points, for the hexagons are displaced in sync, clockwise for the mode IIIa and anti-clockwise for the mode IVa. This should be compared to the atomic displacements in the modes IIIc and IVc, where the atoms belonging to the hexagons move in pairs toward each other. Rotating hexagons in the modes IIIa and IVa produce tension of the valence bonds between the hexagons thus resulting in negative pressure.

Actually, it is well-known that structural units with rotational degrees of freedom can result in appearance of negative properties of materials.[79–82]

4. Conclusions

By the method of molecular dynamics, properties of DNVM in graphene lattice, modeled with the use of the Savin interatomic potentials,[8] were investigated. All 4 one-component and 12 two-component DNVM were analyzed, see Figure 2.

It was shown that one-component DNVM have frequencies mainly within the phonon spectrum of graphene, see Figure 3b. Only DNVM III at amplitudes greater than 0.2Å has frequency slightly above the phonon spectrum. One-component DNVM produce positive in-plane pressure in graphene sheet, see Figure 3c.

Two-component DNVM are composed of two vibrational modes, the main mode and a small addition of one of the four one-component DNVM. More precisely, DNVM Ia to Ie include small-amplitude DNVM I; DNVM II includes small-amplitude DNVM II; DNVM IIIa to IIIc include small-amplitude DNVM III; and DNVM IVa to IVc include small-amplitude DNVM IV. In order to obtain periodic in time motion, amplitudes of the main and additional modes should be properly chosen. If ω is the main mode frequency, then additional small-amplitude mode has frequency 2ω, that is, the second harmonic generation takes place. Some of DNVM, for example, Ia can have second harmonic frequency nearly twice as large as the maximal phonon frequency. Thus, we demonstrate that graphene lattice can support natural nonlinear vibrations at frequencies considerably above the maximal phonon frequency. This effect arises as a result of nonlinearity of interatomic interactions. The amplitude of the second harmonic decreases quadratically with decreasing the main mode amplitude, see Figure 6a.

Two-component DNVM IIIa and IVa produce negative pressure, see Figure 6c because in these two modes carbon hexagons rotate as nearly rigid units.

It is well-known that an isotropic elastic body under negative pressure becomes an auxetic.[83] Since DNVM IIIa and IVa produce negative pressure, it would be interesting to analyze their effect on the elastic properties and particular on auxeticity of graphene. This will be done in a forthcoming work.

Acknowledgements

The work of E.A.K. was supported by the Russian Foundation for Basic Research, grant No. 18-32-20158. S.A.S. acknowledges support by the Ministry of Education and Science of the Russian Federation (state assignment grant No. 12.5425.2017/8.9). G.M.Ch. and D.S.R. acknowledge support by the Ministry of Education and Science of the Russian Federation (state assignment grant No. 3.5710.2017/8.9). The work of E.G.E. was supported by Act 211 Government of the Russian Federation, contract No. 02. A03.21.0011. S.V.D. gratefully acknowledges financial support provided by the Russian Science Foundation, grant No. 14-13-00982. This research was supported by "The Tomsk State University competitiveness improvement programme."

Keywords

delocalized nonlinear vibrational mode, graphene, molecular dynamics, negative pressure, nonlinear dynamics, second harmonic generation

Received: February 11, 2018
Revised: October 21, 2018
Published online: December 3, 2018

[1] A. K. Geim, *Angew. Chem. Int. Ed*. **2011**, *50*, 6966.
[2] K. S. Novoselov, *Angew. Chem. Int. Ed*. **2011**, *50*, 6986.
[3] J. A. Baimova, *J. Micromech. Mol. Phys*. **2017**, *2*, 1750001.
[4] H. Yanagisawa, T. Tanaka, Y. Ishida, M. Matsue, E. Rokuta, S. Otani, C. Oshima, *Surf. Interface Anal*. **2005**, *37*, 133.
[5] M. Mohr, J. Maultzsch, E. Dobardzic, S. Reich, I. Milosevic, M. Damnjanovic, A. Bosak, M. Krisch, C. Thomsen, *Phys. Rev. B* **2007**, *76*, 035439.
[6] W. Pan, J. Xiao, J. Zhu, C. Yu, G. Zhang, Z. Ni, K. Watanabe, T. Taniguchi, Y. Shi, X. Wang, *Sci. Rep*. **2012**, *2*, 893.
[7] S. Mann, R. Kumar, V. K. Jindal, *RSC Adv*. **2017**, *7*, 22378.
[8] A. V. Savin, Y. S. Kivshar, B. Hu, *Phys. Rev. B* **2010**, *82*, 195422.
[9] H. Zhang, G. Lee, K. Cho, *Phys. Rev. B* **2011**, *84*, 115460.
[10] C. A. Polanco, L. Lindsay, *Phys. Rev. B* **2018**, *97*, 014303.
[11] Y. Kuang, L. Lindsay, S. Shi, X. Wang, B. Huang, *Int. J. Heat Mass Tran*. **2016**, *101*, 772.
[12] J. A. Baimova, S. V. Dmitriev, K. Zhou, A. V. Savin, *Phys. Rev. B* **2012**, *86*, 035427.
[13] J. A. Baimova, S. V. Dmitriev, K. Zhou, *Phys. Status Solidi B* **2012**, *249*, 1393.
[14] E. A. Korznikova, S. V. Dmitriev, *J. Phys. D: Appl. Phys*. **2014**, *47*, 345307.
[15] X. Gao, C. Li, Y. Song, T.-W. Chou, *Comput. Mater. Sci*. **2017**, *135*, 152.
[16] Y.-L. Ma, B.-Q. Li, *Physica A* **2018**, *494*, 169.
[17] Y. Yamayose, Y. Kinoshita, Y. Doi, A. Nakatani, T. Kitamura, *Europhys. Lett*. **2007**, *80*, 40008.
[18] L. Z. Khadeeva, S. V. Dmitriev, Yu. S. Kivshar, *JETP Lett*. **2011**, *94*, 539.
[19] Y. Doi, A. Nakatani, *Proc. Eng*. **2011**, *10*, 3393.
[20] Y. Doi, A. Nakatani, *J. Solid Mech. Mater. Eng*. **2012**, *6*, 71.
[21] T. Shimada, D. Shirasaki, T. Kitamura, *Phys. Rev. B* **2010**, *81*, 035401.
[22] I. P. Lobzenko, G. M. Chechin, G. S. Bezuglova, Yu. A. Baimova, E. A. Korznikova, S. V. Dmitriev, *Phys. Solid State* **2016**, *58*, 633.
[23] E. Barani, I. P. Lobzenko, E. A. Korznikova, E. G. Soboleva, S. V. Dmitriev, K. Zhou, A. M. Marjaneh, *Eur. Phys. J. B* **2017**, *90*, 38.
[24] A. Fraile, E. N. Koukaras, K. Papagelis, N. Lazarides, G. P. Tsironis, *Chaos Soliton. Fract*. **2016**, *87*, 262.
[25] V. Hizhnyakov, M. Klopov, A. Shelkan, *Phys. Lett. A* **2016**, *380*, 1075.
[26] V. Hizhnyakov, A. Shelkan, M. Haas, M. Klopov, *Lett. Mater*. **2016**, *6*, 61.
[27] E. A. Korznikova, J. A. Baimova, S. V. Dmitriev, *Europhys. Lett*. **2013**, *102*, 60004.
[28] S. V. Dmitriev, J. A. Baimova, E. A. Korznikova, A. P. Chetverikov, *Nonlinear Systems*. Vol. 2. Understanding Complex Systems. (Eds: J. Archilla, F. Palmero, M. Lemos, B. Sanchez-Rey, J. Casado-Pascual) Springer, Cham **2018**, p. 175.
[29] E. Barani, E. A. Korznikova, A. P. Chetverikov, K. Zhou, S. V. Dmitriev, *Phys. Lett. A* **2017**, *381*, 3553.
[30] R. T. Murzaev, D. V. Bachurin, E. A. Korznikova, S. V. Dmitriev, *Phys. Lett. A* **2017**, *381*, 1003.
[31] S. V. Dmitriev, E. A. Korznikova, Yu. A. Baimova, M. G. Velarde, *Phys. Usp*. **2016**, *59*, 446.
[32] S. V. Dmitriev, *J. Micromech. Mol. Phys*. **2016**, *1*, 1630001.
[33] I. Evazzade, I. P. Lobzenko, E. A. Korznikova, I. A. Ovid'ko, M. R. Roknabadi, S. V. Dmitriev, *Phys. Rev. B* **2017**, *95*, 035423.
[34] I. Evazzade, I. P. Lobzenko, D. Saadatmand, E. A. Korznikova, K. Zhou, B. Liu, S. V. Dmitriev, *Nanotechnology* **2018**, *29*, 215704.
[35] (a) V. P. Sakhnenko, G. M. Chechin, *Dokl. Akad. Nauk* **1993**, *330*, 308; (b) V. P. Sakhnenko, G. M. Chechin, *Phys. Dokl*. **1993**, *38*, 219.
[36] G. M. Chechin, V. P. Sakhnenko, *Physica D* **1998**, *117*, 43.
[37] (a) V. P. Sakhnenko, G. M. Chechin, *Dokl. Akad. Nauk* **1994**, 338, 42; (b) V. P. Sakhnenko, G. M. Chechin, *Phys. Dokl*. **1994**, *39*, 625.
[38] G. Chechin, D. Ryabov, S. Shcherbinin, *J. Micromech. Mol. Phys*. **2018**, *3*, 1850002.
[39] G. Chechin, D. Ryabov, S. Shcherbinin, *Lett. Mater*. **2017**, *7*, 367.
[40] E. A. Korznikova, S. Y. Fomin, E. G. Soboleva, S. V. Dmitriev, *JETP Lett*. **2016**, *103*, 277.
[41] V. M. Burlakov, S. A. Kiselev, V. I. Rupasov, *Phys. Lett. A* **1990**, *147*, 130.
[42] Yu. S. Kivshar, M. Peyrard, *Phys. Rev. A* **1992**, *46*, 3198.
[43] T. Cretegny, S. Ruffo, A. Torcini, *Physica D* **1998**, *121*, 109.
[44] T. Dauxois, R. Khomeriki, F. Piazza, S. Ruffo, *Chaos* **2005**, *15*, 015110.
[45] K. Ikeda, Y. Doi, B.-F. Feng, T. Kawahara, *Physica D* **2007**, *225*, 184.
[46] L. Z. Khadeeva, S. V. Dmitriev, *Phys. Rev. B* **2010**, *81*, 214306.
[47] E. A. Korznikova, D. V. Bachurin, S. Y. Fomin, A. P. Chetverikov, S. V. Dmitriev, *Eur. Phys. J. B* **2017**, *90*, 23.
[48] S. V. Dmitriev, E. A. Korznikova, D. I. Bokij, K. Zhou, *Phys. Status Solidi B* **2016**, *253*, 1310.
[49] K. V. Tretiakov, K. W. Wojciechowski, *Phys. Status Solidi B* **2013**, *250*, 2020.
[50] J. N. Grima, S. Winczewski, L. Mizzi, M. C. Grech, R. Cauchi, R. Gatt, D. Attard, K. W. Wojciechowski, J. Rybicki, *Adv. Mater*. **2015**, *27*, 1455.
[51] K. L. Alderson, A. Alderson, J. N. Grima, K. W. Wojciechowski, *Phys. Status Solidi B* **2014**, *251*, 263.
[52] A. Alderson, *Chem. Ind*. **1999**, *17*, 384.
[53] K. E. Evans, A. Alderson, *Adv. Mater*. **2000**, *12*, 617.
[54] K. L. Alderson, V. R. Simkins, V. L. Coenen, P. J. Davies, A. Alderson, K. E. Evans, *Phys. Status Solidi B* **2005**, *242*, 509.
[55] R. H. Baughman, J. M. Shacklette, A. A. Zakhidov, S. Stafstrom, *Nature* **1998**, *392*, 362.
[56] S. P. Tokmakova, *Phys. Status Solidi B* **2005**, *242*, 721.
[57] A. Norris, *Proc. Roy. Soc. A* **2006**, *462*, 3385.
[58] T. Paszkiewicz, S. Wolski, *Phys. Status Solidi B* **2007**, *244*, 966.
[59] T. Paszkiewicz, S. Wolski, *J. Phys.: Conf. Ser*. **2008**, *104*, 012038.
[60] A. C. Branka, D. M. Heyes, K. W. Wojciechowski, *Phys. Status Solidi B* **2009**, *246*, 2063.

[61] R. V. Goldstein, V. A. Gorodtsov, D. S. Lisovenko, *Mech. Solids* **2010**, *45*, 529.
[62] R. V. Goldstein, V. A. Gorodtsov, D. S. Lisovenko, *Dokl. Phys*. **2011**, *56*, 399.
[63] A. C. Branka, D. M. Heyes, K. W. Wojciechowski, *Phys. Status Solidi B* **2011**, *248*, 96.
[64] A. C. Branka, D. M. Heyes, Sz. Mackowiak, S. Pieprzyk, K. W. Wojciechowski, *Phys. Status Solidi B* **2012**, *249*, 1373.
[65] R. V. Goldstein, V. A. Gorodtsov, D. S. Lisovenko, *Phys. Status Solidi B* **2013**, *250*, 2038.
[66] V. V. Krasavin, A. V. Krasavin, *Phys. Status Solidi B* **2014**, *251*, 2314.
[67] R. V. Goldstein, V. A. Gorodtsov, D. S. Lisovenko, M. A. Volkov, *Lett. Mater.* **2015**, *5*, 409.
[68] R. V. Goldstein, V. A. Gorodtsov, D. S. Lisovenko, M. A. Volkov, *Phys. Mesomech*. **2013**, *16*, 13.
[69] D. S. Lisovenko, J. A. Baimova, L. Kh. Rysaeva, V. A. Gorodtsov, A. I. Rudskoy, S. V. Dmitriev, *Phys. Status Solidi B* **2016**, *253*, 1295.
[70] J. N. Grima, R. Caruana-Gauci, K. W. Wojciechowski, K. E. Evans, *Smart Mater. Struct*. **2013**, *22*, 084015.
[71] T. Strek, H. Jopek, E. Idczak, K. W. Wojciechowski, *Materials* **2017**, *10*, 1386.
[72] L. L. Hu, M. Z. Zhou, H. Deng, *Composites* **2019**, *207*, 323.
[73] D. Rayneau-Kirkhope, *Sci. Rep*. **2018**, *8*, 12437.
[74] L. D'Alessandro, V. Zega, R. Ardito, A. Corigliano, *Sci. Rep*. **2018**, *8*, 2262.
[75] D. D. Nguyen, C. H. Pham, *J. Sandw. Struct. Mater.* **2018**, *20*, 692.
[76] X.-T. Wang, B. Wang, Z.-H. Wen, L. Ma, *Compos. Sci. Technol*. **2018**, *164*, 92.
[77] H. Zhang, Y. Luo, Z. Kang, *Compos. Struct*. **2018**, *195*, 232.
[78] R. D. Skeel, G. Zhang, T. Schlick, *SIAM J. Sci. Comput*. **1997**, *18*, 203.
[79] J. N. Grima, R. Gatt, A. Alderson, K. E. Evans, *J. Phys. Soc. Jpn* **2005**, *74*, 2866.
[80] D. Attard, J. N. Grima, *Phys. Status Solidi B* **2008**, *245*, 2395.
[81] D. Attard, J. N. Grima, *Phys. Status Solidi B* **2012**, *249*, 1330.
[82] E. Chetcuti, B. Ellul, E. Manicaro, J. P. Brincat, D. Attard, R. Gatt, J. N. Grima, *Phys. Status Solidi B* **2014**, *251*, 297.
[83] K. W. Wojciechowski, *Mol. Phys. Rep*. **1995**, *10*, 129.